Journal of Physics: Conference Series **767** (2016) 012014 doi:10.1088/1742-6596/767/1/012014

The Role of Particle Drifts in the Heliosphere

József Kóta

The University of Arizona, Lunar and Planetary Laboratory, Tucson, AZ 8521-0092, USA

E-mail: kota@lpl.arizona.edu

Abstract. Some of the basic effects of particle drifts on cosmic rays in the inner and outer Heliosphere are discussed. We bring arguments supporting that particle drifts, convection and adiabatic cooling can be treated by the same matching condition at discontinuities, the apparent infinite value of drift speed is consistent with the diffusive description. Simple illustrative examples are presented to highlight the differences between drift and no-drift solutions of the Parker equation. A simplistic model simulation is presented to demonstrate the role of drifts in the 22-year solar modulation cycle. The nature and possible effects of drift in the heliosheath are briefly addressed.

1. Introduction

It was 40 years ago that the two Voyager spacecraft started their amazing journey through our Heliosphere and beyond. It is quite a remarkable coincidence that two major developments in the theory of energetic charged particles were launched almost the same time. Diffusive shock acceleration (DSA) was proposed in 1977 (Axford et al., 1977; Bell et al., 1978; Blandford and Ostriker, 1978; Krymskii 1977) and it was in the same year that Jokipii et al. (1977) called attention to the profound role particle drifts play in the transport of cosmic rays. The 2×40=80 years of Voyager mission, with the leadership of Edward Stone, brought many fundamental observations inspiring further research, and hopefully this shall continue for many more years to come.

While the idea of DSA was immediately embraced, the concept of particle drifts met some resistance in the cosmic ray community. A beautiful observation of Voyagers bringing compelling evidence for the action of drifts meant a milestone in 1987. Comparing V1, V2 and Pioneer 10 measurements, Cummings et al. (1987) found that, the intensity of anomalous oxygen was decreasing away from the flat heliospheric current sheet (HCS). This occurred during the so called $A < 0$ solar minimum, in agreement with the prediction of drift models (Jokipii, 1986) This observation demonstrated the effects of both the DSA and particle drifts at the same time.

The present work is devoted to cosmic-ray effects connected with particle drift. Drifts are important both in the acceleration and spatial transport of energetic particles. We shall focus on the solar modulation of anomalous and galactic cosmic rays (ACRs and GCRs), examples will be brought for GCRs. Sections 2 and 3 reiterate some general features of drift effects and illustrative examples are presented for the simplest 2-dimensional (2D)convection-diffusion model. Section 4 presents a simplistic simulation model of the 22-year solar cycle focusing on drift effects and omitting other important mechanisms of GCR modulation. Finally the nature and possible role of particle drifts in the heliosheath is briefly addressed in Section 5.

2. Drift effects on cosmic rays in the Heliosphere

The most widely used tool describing the diffusive transport of energetic charged particles in the heliospheric magnetic field (HMF) is the equation of Parker (1965). This robust equation assumes that scattering is frequent enough to maintain quasi-isotropic particle distribution. Then the omnidirectional phase-space density $f(x_i, p, t)$ at position, x_i, momentum, p, and time, t obeys

$$\frac{\partial f}{\partial t} = \frac{\partial}{\partial x_i}\Big(\kappa_{ij}\frac{\partial f}{\partial x_j}\Big) - V_i\frac{\partial f}{\partial x_i} + \frac{1}{3}\frac{\partial V_i}{\partial x_i}\frac{\partial f}{\partial ln\, p} + Q \tag{1}$$

where the consecutive terms represent diffusion, advection by the solar wind moving at velocity, V_i, and adiabatic energy change due to the expansion or compression of the fluid. Energy and momentum are measured in the frame of the fluid. $Q(x_i, p, t)$ on the RHS accounts for possible sources, or sinks. Double indices refer to summation. The full 3D diffusion tensor, κ_{ij} contains an anti-symmetric component, κ^a_{ij}, which accounts for regular particle motion in the large-scale HMF, and whose divergence yields the drift velocity, V_i^{dr}, in the non-uniform HMF.

$$\kappa^a_{ij} = \kappa_A \epsilon_{ijk} b_k \qquad\qquad V_i^{dr} = \frac{\partial \kappa^a_{ij}}{\partial x_j} \tag{2}$$

For weak scattering, $\kappa_A = r_g v/3 = Pv/3B$ where r_g stands for the gyroradius of a particle of speed, v, and rigidity, P. $b_i = B_i/B$ is a unit vector along the magnetic field, B_i. The drift motion, V_i^{dr}, is frequently treated as a separate term, then only the symmetric part of κ_{ij} is kept in Eq. (1). For an excellent review on the Parker equation see Moraal (2013).

Modulation, in most cases, is connected with energy change. In a static magnetic field, drift would be present but, in itself, would not cause density gradients, anisotropy or energy change. In a moving fluid, on the other hand, drifts do affect energy change, by virtue of controlling the path and dwelling time of GCRs in the heliosphere. A conceptual problem is posed by particle drifts at current sheets, shocks, or other discontinuities, where drift derived form Eq. (2) can be infinitely fast. A great deal of work has been done on this subject. Isenberg and Jokipii (1979) pointed out that the standard form of drifts applies under broad conditions. Other efforts substitute the step-like discontinuity by a sharp but continuous change of κ_A, hence distribute the drift over a finite thickness (Burger et al., 1985).

We note that the Parker equation can also be re-written in a more compact form as

$$\frac{\partial f}{\partial t} = \frac{1}{p^3}\frac{\partial}{\partial \xi_a}\Big(p^3\, K_{ab}\frac{\partial f}{\partial \xi_b}\Big) + Q \qquad\qquad a, b = 1, ..., 4 \tag{3}$$

where ξ_a is a 4D vector comprising of the three spatial coordinates, x_i, with $\xi_4 = lnp^3 = 3\, lnp$ added as the 4th component. The corresponding 4D diffusion tensor is

$$K_{ab} = \begin{pmatrix} \kappa_{ij} & V_j \\ -V_i & 0 \end{pmatrix} \qquad\qquad i, j = 1, 2, 3 \tag{4}$$

This implies that, at least technically, there is no essential difference between advection, energy loss, and drift, all being derived from the anti-symmetric part of the 4×4 diffusion tensor. In general, regular reversible motion appears in the antisymmetric part, while diffusive irreversible motion is in the symmetric part of the 4D diffusion tensor. A purely anti-symmetric tensor has imaginary eigenvalues corresponding to reversible motion. The form of Eq. (3) suggests that drifts, advection and energy change are best treated in the same way at discontinuities. The normal component of $K_{ab}\, \partial f/\partial \xi_b$ should match at the two side of the discontinuity:

$$n_i(\kappa_{ij}\frac{\partial f}{\partial x_j} + V_i\frac{\partial f}{\partial ln\, p^3}\Big)\Big|_1^2 = 0 \tag{5}$$

which indicates that the use of matching condition (5) is sufficient and there is no compelling reason to distribute the drift over a finite thickness. These two approaches may differ in subtleties but they should give very much the same results.

Finally we note that the infinite value of drift velocity is not an inconsistency in a diffusive description. Diffusion equation is a robust approximation which takes the limit of infinitely fast particle speed and infinitely small diffusion mean free path, keeping the product finite. This shows up in a number of features of the diffusive equation. It is known that, in diffusive solutions, particles appear instantly (though with little chance) at large distances. Similarly, the frequently used $f = 0$ condition at absorbing boundaries implies an infinite particle speed. One further example is DSA. The diffusion solution implies an infinite number of shock crossings with infinitesimal energy gain at each crossing. All these give good approximation as long as the conditions of diffusive transport hold, and break down where the diffusive description is no longer valid.

3. Simple illustrative examples

To illustrate the basic drift effects imagine a 2D (x,z) slab model with the fluid velocity, V_i, pointing in the x direction, and the magnetic field pointing in the ignorable y direction. In an analogy to GCR modulation, x and z may play the role of radius and latitude, respectively. For brevity, assume that both V_i and κ_{ij} are uniform in space. This represents a case when modulation takes place without energy change, and Parker's equation reduces to a convection-diffusion equation which has the obvious solution

$$f_0(x_i) \propto exp\Big(Vx/\kappa_{xx}\Big) \qquad g_x = \frac{\partial ln(f)}{\partial x} = V/\kappa_{xx} \tag{6}$$

There are other, z dependent solutions, which may appear if we impose a z-dependent boundary condition. These solutions do, however decay faster and f_0 dominates at large distances from outer boundary.

The z-independent solution, f_0, involves a unobstructed streaming in the positive or negative z direction depending on the sign of B_y. This changes if we place reflecting boundaries or periodic currents sheets (their effect are the same for this case) at say $z = 0$ and $z = z_0$. Then particles drift along the current sheets (or reflecting boundaries) and the solution changes to (Kóta, 1981)

$$f_0^\star(x_i) \propto exp\Big(x_i\kappa_{ij}^{-1}V_j\Big) \qquad g_x^\star = V/(\kappa_{xx} + \kappa_A^2/\kappa_{zz}) = V/\kappa^\star \tag{7}$$

where $f_0^\star$ is a completely isotropic solution. Eq. (7) indicates that drifts will reduce the gradients in the x direction, and this reduction depends on the value of the latitudinal diffusion coefficient κ_{zz}. Roughly speaking, drift assists GCRs to find a faster way into the heliosphere, hence reduce modulation. GCRs follow the fast drift path as long as κ_{zz} is small, but larger values of κ_{zz} destroys the coherent drift pattern (Kóta, 1989; 2013).

We note that, results were similar for an oblique magnetic field, the effective $\kappa^\star$ would be somewhat modified, and an anisotropy, analogous to the co-rotational anisotropy, could also appear in the y direction.

Figure 1 shows numerical solutions with keeping $\kappa_{xx} = \kappa_{xz} = -\kappa_{zx} = \kappa_A$ constant. The important dimensionless parameter is $\eta = \kappa_A^2/(\kappa_{xx}\kappa_{zz})$. We find that, after some transient regime near the outer boundary, the solutions settle to a fully isotropic solution given by Eq. (7). A larger value of η implying smaller 'latitudinal' diffusion gives milder modulation relative to the 1D 'no-drift' solution of (6).

To demonstrate the effect of a wavy HCS, we present a simulation carried out with a sectored field placed between two reflecting boundaries at $z = -z_0$ and $z = +z_0$. A simple step-function is used, the sectored field extends from $-0.5z_0$ to $+0.5z_0$. The simulation presented in Figures

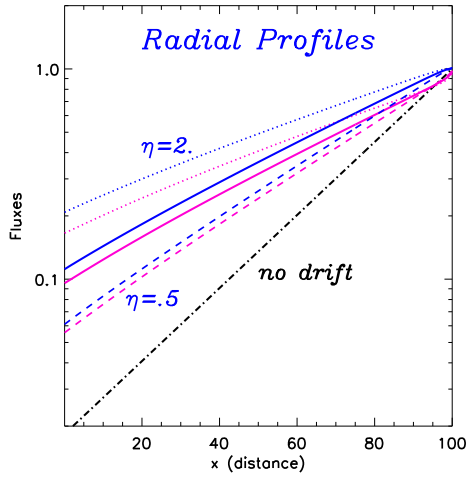

Figure 1. Solution of the 2D convection-diffusion equation. Shown are drift solutions with $\eta = 0.5$ (dashed), $\eta = 1.0$ (solid), and $\eta = 2.0$ (dotted). Blue lines refer to positions at $z = 0$, magenta lines refer to $z = z_0$. Smaller κ_{zz} (larger η) values results in less modulation. Drift solutions always result in less modulation than the no-drift solution (black dashed-dotted line).

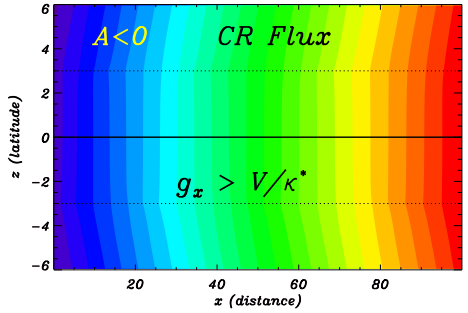

Figure 2. Color plot of GCR density (red high, blue low) obtained with sectored HCS extending between the dotted lines. Note that the latitudinal (z) gradients essentially vanish in the sectored area. Radial x) gradients and modulation increase with the increase of the latitudinal extent of the HCS.

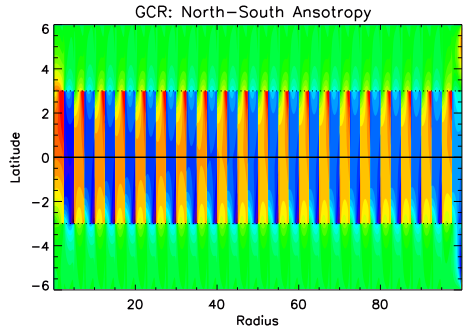

Figure 3. Color plot of cosmic-ray streaming in the z (latitudinal) direction in a sectored field. 'N-S' anisotropies arise, which alternate between upward (red) and downward (blue) directions according to the polarity of the respective sector. Anisotropies are small at higher latitudes in the unipolar region (green).

2 and 3 use $\eta = 1.0$ and the same other parameters used previously (Fig. 1), the only difference is the inclusion of a sectored field.

Inspection of Figure 2 showing the predicted spatial distribution of GCRs, indicates that the 'latitudinal' (z) gradient does essentially vanish in the sectored area (between the dotted lines). The radial gradient increases, the radial variation moves toward the 'no-drift' solution. What happens is that drift along the HCS allows a fast latitudinal transport, the effect of which is the same as that of a larger κ_{zz}.

An important consequence of the sectored field is the rise of N-S streaming in the z or $-z$ direction depending on the polarity of the respective sector. This is seen in Figure 3. The presence of this sector-dependent N-S anisotropy has been long known and been widely used to infer the local radial gradient. Studies of the GCR anisotropies offer a unique tool to obtain

constraints on the local transport parameters (see for instance Bieber and Chen, 1991; Chen and Bieber, 1993; Gil et al., 2012; Munakata et al., 2014). The modeling of GCR anisotropies requires fully 3D simulations including the proper κ_A parameter. The presence of the N-S anisotropy seems to indicate that drift is present even during solar maxima, but global drift effects are reduced due to the fast latitudinal transport. In other words, drift effects do diminish without scaling down the anti-symmetric component of the full diffusion tensor.

4. 22-year solar modulation cycle of GCRs

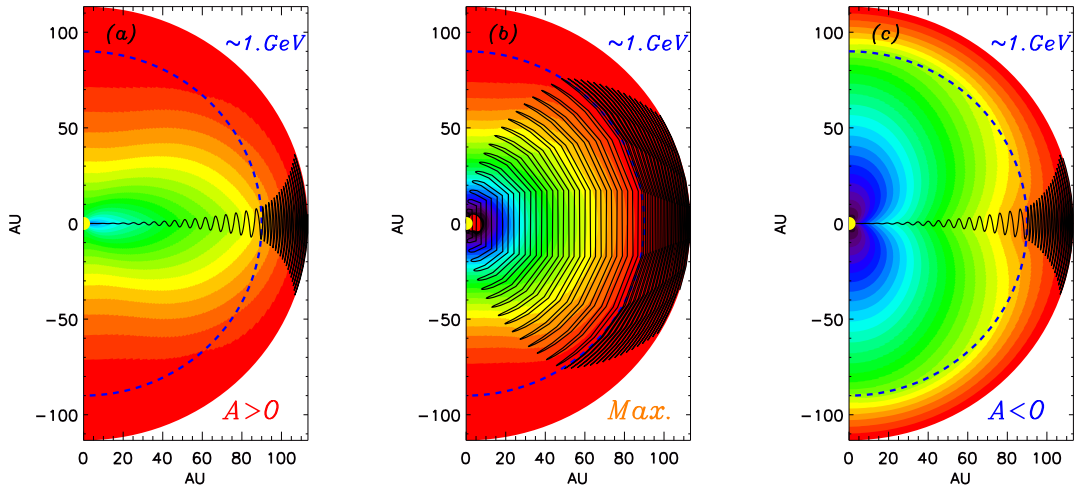

Figure 4. Contour-plots of GCR intensity at $A > 0$ solar minimum (a), near solar maximum (b), and at $A < 0$ solar minimum (c). Red means high, blue means low intensities. The TS is shown by the dashed circle, the wavy black lines indicate the evolving HCS. Note the different latitudinal variation during the two solar minima of opposite polarities.

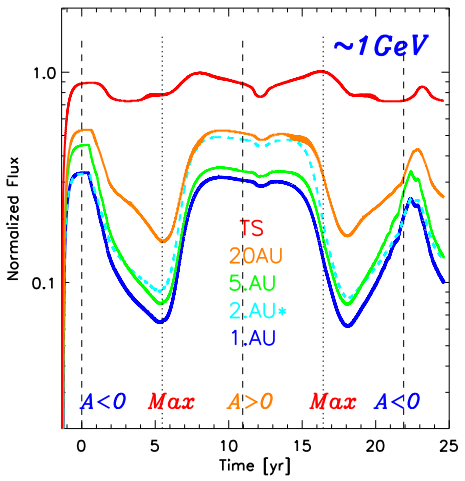

Figure 5. 22-year solar-cycle variation of ∼1GeV GCR intensity at different heliocentric radii in the Heliosphere. All curves refer to the equatorial plane except for the 2AU curve, which refers to high latitude. Vertical lines mark times when the tilt angle at the Sun is 0^o (dashed) or 90^o (dotted). GCR fluxes follow the changing tilt with some delay.

In this section we present a simplistic simulation using an axially symmetric model to highlight the role of particle drifts in the 22-year cycle solar modulation of GCRs. We focus on the effects connected with the polarity reversal of the solar magnetic field and the changes in the tilt angle

of the heliospheric current sheet (HCS) dividing the two hemishperes of opposite polarities. Other important aspects of the modulation process, such as the cyclic variation of solar wind speed, magnetic field strength and diffusion coefficients are not included here, so results are illustrative and are not intended to fit observations.

We consider a spherical supersonic solar wind with a uniform radial speed of $400km/s$, which undergoes a shock transition at the termination shock (TS) placed at 90AU heliographic radius. The solar wind speed is reduced at the TS by a factor of 3, and is kept to flow radially as an incompressible fluid ($V \propto 1/r^2$). An artificial outer boundary is imposed at ≈115 AU, where the GCR flux is set equal to the presumed interstellar spectrum of Webber and Higbie (2009).

We note that, under broad conditions, a stable corotation yields a HMF

$$B_i = \Big(\frac{B_0}{n_0 V_0)}\Big)\, n\, (V_i - \epsilon_{ijk}\Omega_j x_k) \tag{8}$$

where Ω_j stands for the rotation of the Sun, and the factor $(B_0/n_0 v_0)$ remains constant along each magnetic field line carried by the solar wind. A temporal change in the HCS introduces a more complex HMF, and an additional meridional component appears inevitably. Modeling the effects of sectored HMF requires 3D simulations (Kóta and Jokipii, 1983, 1991; Hattingh and Burger, 1995). Potgieter and Moraal (1985) developed a 2D model that captured the modulating effects of the wavy HCS. This method has been successfully applied in a sequence of work to reconstruct the variation spatial and temporal variation of GCRs (see Burger and Potgieter, 1989; Burger and Hattingh 1995, Potgieter, 2013).

Here we take the simplistic approach: in calculating drifts we omit the radial component of the HMF, which is important in the inner heliosphere but its relative role decreases fast toward larger distances from the Sun. Magnetic field lines shall be assumed to be hoops that are passively carried by the wind:

$$B_i = -\Big(\frac{B_0 n}{n_0 V_0)}\Big)\epsilon_{ijk}\Omega_j x_k \tag{9}$$

For a uniform radial wind speed the azimuthal field decreases as $\propto n * \rho$, where $\rho = rcos(\Theta)$ is the distance from the Sun's rotation axis at latitude, Θ. The polarity is preserved from the time $t - r/V$, when the ring originated from the Sun. The virtue of this field model is that it is less restrictive than the full spiral, and allows the continuous change of the tilt angle without changing the geometry of the field.

The parallel mean free path, $\lambda_{||}$, is conveniently assumed to be proportional to particle rigidity, P, and inversely proportional to the local magnetic field so that 1 GV particles in a 6 nT field have $\lambda_{||} = 0.075$AU. A relatively low value of $\kappa_\perp/\kappa_{||} = 0.02$ is chosen to highlight drift effects, a larger value of $\kappa_\perp$ would reduce these to some extent.

The spiral field (8) becomes weak near the poles, so the polar region is dominated by randomly oriented transverse fields (Jokipii and Kóta, 1989). We add a random transverse component to the field at all latitudes with $\delta B_t = \delta B_0 (n\, r)/(n_0 r_0)$, so that $(\delta B/B) \approx 0.2$ at the Earth. In calculating the field strength and the diffusion coefficients we include the full spiral field together with the contribution of the random component. The random dB_t component tends to reduce the radial and enhance the latitudinal diffusion.

Figure 4 shows three phases of the 22-year solar cycle. The successive panels depict the spatial distribution of $\sim 1GV$ GCRs around $A > 0$ solar minimum (a), near solar maximum (b) and $A < 0$ solar minimum (c). The robust drift features are clearly visible, the latitudinal dependence of GCRs is markedly different at consecutive solar minima. GCRs find easier to penetrate into the inner heliosphere through the polar region in the $A > 0$ solar minimum, and along the near flattened equatorial HCS in the $A < 0$ minimum. The distribution is largely spherical with small latitudinal gradients when the HCS is highly tilted around solar maximum.

Figure 5 shows the 22-year cycle caused solely by the changing tilt of the HCS, as predicted for different locations in the Heliosphere. All curves refer to equatorial locations except for the dashed $2AU^{\star}$ curve, which refers to high latitude and predicts a distinctly different profile. The familiar peaked and plateau GCR maxima are clearly visible. GCRs follow the change of tilt with some delay since the flattening of the HCS takes time to propagate to the outer heliosphere. Inspection of Fig. 5 also indicates that the momentary tilt angle, in itself, cannot be used as a single parameter to determine the level of modulation. Modulation is weakest and GCR fluxes are the highest when the HCS is flat in the whole computational domain. This is apparent in the asymmetry between year 0 and year 22. The momentary tilt is 0^o in both cases, but a flat HCS was assumed for the whole period between years 0 and = 1.5 (when numerical simulation was started with an empty heliosphere).

No drift solutions would be horizontal lines through the GCR fluxes at solar maxima. The calculations presented here were using a relatively small value of $\kappa_{\perp}$ in order to emphasize drift effects. The low value of $\kappa_{\perp}$ enhances the GCR flux at the $A < 0$ solar minimum, while has less effect during the $A > 0$ cycle. Global drift effects diminished during solar maxima without any change in the value of κ_A.

5. Drifts in the Heliosheath

The diffusion and drift motion of cosmic rays in the heliosheath critically depends on the structure of the HMF beyond the TS. Currently there are two different views on the global structure of the heliosheath. The traditional view has been that a long heliotail is formed in the direction of the interstellar wind. Because of the slow radial speed of the subsonic wind in the nose section, magnetic sectors in this model become closely stacked and may become essentially transparent for GCR whose gyro-radii are comparable or larger than the width of the magnetic sectors (Florinski, 2011). Further away from the TS, the HCS becomes completely distorted and disintegrates due to the shear of the flow (Pogorelov et al., 2015 and references therein).

Recently Opher et al. (2015) proposed an alternative 'croissant ' model suggesting that, the magnetic tension causes the solar fluid to be lifted southward and northward forming a pair of jets, and this avoids the further stretching of field lines. Drake et al. (2015) gave a simple model to illustrate the physics involved in the jet model. The omission of interstellar wind and interstellar magnetic field allowed these authors to construct an axially symmetric model. Furthermore, the omission of the radial component of the HMF, which has negligible role in the dynamics, led to a HMF where field lines are hoops carried by the solar wind.

Figure 6 depicts a schematic picture of the HMF in this simplified jet model. The left panel (a) shows the hoop-like field lines directed oppositely on the two sides of the flat HCS. The magnetic field for this case is given by Eq (9). We note that retaining the radial field component Eq. (8) would hold, the omitted field component would remain directed along the stream lines, and be proportional to $n\,V_i$.

The right panel (b) shows a meridional cut allowing a wavy HCS. The structure of the HCS is distorted due to the shear of the fluid but to a lesser extent than the distortion in the 'classic' long-heliotail case. The width and placement of the wavy HCS are not in scale, the HCS is drawn largely stretched in Fig. 6 for brevity.

The particle drift, V_i^{dr} can be readily obtained. Taking the weak scattering limit, the resulting drift in this model of magnetic hoops is

$$V_i^{dr} = \epsilon_{ijk}\frac{vP\,B_k}{3B^2}\frac{\partial}{\partial x_j}\Big(ln(\frac{B_0}{n_0V_0}) + ln\,n\Big) \tag{10}$$

In the simplest approximation the factor $B_0/(n_0V_0)$ can be taken as constant except for its sign which changes at the HCS. Then, the first term in Eq. (10) gives the the inward drifts along the HP and the HCS, which is balanced by an outward drift concentrated at the polar line.

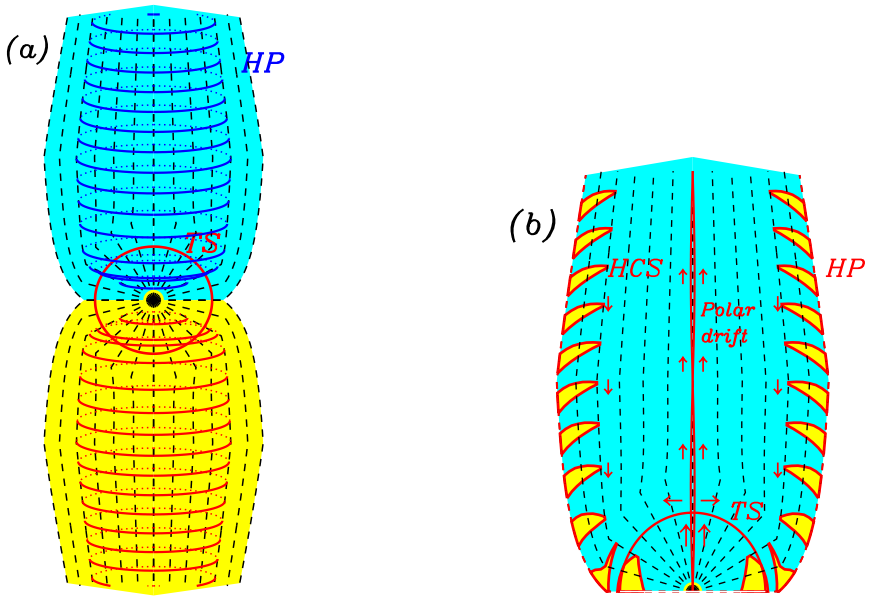

Figure 6. Schematic view of an axially symmetric toy-model of the Heliosphere similar to that of Drake et al. (2015). The left panel (a) shows that the solar wind is deflected to form a pair of jets. Magnetic field lines are oppositely directed hoops below and above the helioequatorial plane. The right panel (b) depicts a schematic view with a tilted HCS in the Northern meridional section. Red arrows indicate the direction of particle drifts for the $A < 0$ polarity state. The extension of the stretched HCS is not in scale. (see text).

The second term of Eq. (10) has no contribution in the the heliosheath where the density, n, is assumed to be constant. This term yields an equatorward drift along the TS where the density, n, has a jump. These directions refer to the $A < 0$ polarity state, and would reverse for the opposite $A > 0$ state.

The inclusion of random transverse field component, δB_t, is complicated by the velocity shear in the heliosheath, which will stretch and increase this component beyond the TS (in addition to the increase by the compression at the TS). The magnitude of this increase requires further study.

Finally we note that drift along the wavy HCS can provide fast particle transport normal to the stream lines. This can potentially be important for the $A > 0$ polarity case when GCR ions drift inward at the poles. Most of the early models of GCR modulation imposed an artificial boundary some distance from the Sun. The simulation presented in the previous section also suffers from this inherent problem: the polar line offers an easy access for GCRS from the heliopause to the inner heliosphere. In fact, the polar field lines do not to connect the HP, so the question remains how GCR reach the polar regions (Kóta, 2013). We suggest that this could be assisted by drifts along the HCS in a sectored heliosheath. To answer this question requires advanced simulations incorporating the full heliosphere (see Florinski and Pogorelov, 2009; Florinski et al. 2013; Lou et al., 2013; Strauss et al., 2013) and further theoretical research is needed to explore how GCR enter the heliosphere. A surprising finding of the HP crossing of Voyager-1 was the ≈ 20 percent increase seen is the $\sim 200GeV$ GCR flux (Stone et al., 2013; Krimigis et al., 2013). It will be exciting to see if the same intensity jump is repeated at the HP crossing of Voyager-2.

6. Conclusions

Particle drifts are important in both the propagation and acceleration of energetic particles. This work focused on some aspects of drifts in the solar modulation of cosmic rays. Simple numerical simulations were presented to illustrate drift effects, our examples served to highlight the role of drifts and were not intended to fit observations.

Drifts can be derived from the anti-symmetric term of the full 3D diffusion tensor, κ^a_{ij}, hence we may obtain infinitely fast drift speed at discontinuities, such as the HCS or shocks. We argue that this apparently infinite speed does not pose a conceptual problem, the diffusive approach does already represent a limit of infinite particle speed. The Parker equation (1) can be re-cast into a compact form, where drifts, advection, and adiabatic energy change are all derived from the anti-symmetric component of a 4×4 diffusion tensor, which makes it plausible to use the same mathematical treatment and same matching condition for all these quantities. The frequently used method of spreading drift over a finite area is another possible way, the two approaches should give very much the same results.

We re-iterate that global drift effects critically depend on the latitudinal diffusion (Kóta, 1989). Well organized drift motion can occur as long as $\kappa_A \geq \kappa_\perp$. Large $\kappa_\perp$, on the other hand, destroys the coherent drift motion and results in larger radial gradients, i.e. stronger modulation. This will happen without any change in the value of either κ_A or $\kappa_\perp$. Drift along a highly tilted HCS allows fast latitudinal spread of GCRs, which acts in the same way as a larger $\kappa_\perp$ does.

In turbulent magnetic fields, we expect some reduction of κ_A relative to its weak scattering limit (Giacalone et al.; 1999, Minnie et al., 2007). Anisotropy measurements do, however, indicate that this reduction cannot be very strong: a polarity dependent N-S anisotropy connected with radial gradient and anti-symmetric diffusion is clearly seen in neutron monitor data even during solar maxima (Bieber and Chen, 1991). The presence of this anisotropy component would be hard to explain without a substantial value of κ_A. Simulation models should explain both GCR intensities and anisotropies at the same time. This is a challenging task, requiring advanced 3D simulations.

A simplistic model was presented to simulate the 22-year solar modulation cycle of GCRs solely due to the changing tilt of the HCS. We tried to capture the effect of the HCS in an axially symmetric model, where the tilt of the evolving HCS was the sole parameter to vary in time. All other parameters were kept unchanged. The robust features of drift solution, such as the peaked/plateau intensity maxima of GCRs during consecutive 11-year cycles and low fluxes during solar maxima were qualitatively reproduced. This again suggests that global drift effects tend to diminish even without scaling down κ_A during solar maxima.

The possible role of drifts in the heliosheath was briefly touched. While the traditional elongated heliosphere with along heliotail is likely to have a fragmented sector structure, the jet-model of Opher et al (2015) may retain a more coherent magnetic structure where large scale drifts could play a role. Particle drift can certainly be expected along the surface of the HP. We suggest that current sheet drift might play a role in transporting GCRs toward the polar regions during $A > 0$ polarity cycles. It is not inconceivable that HCS reaching the HP or close to the HP can act as cracks where GCRs find easier to penetrate and fill up the heliosphere. The anticipated HP crossing of Voyager-2 may shed light on this question.

Acknowledgments

The author benefited from discussions with J.R. Jokipii and M. Krainev. This work was partially supported by NASA under Grants NNX15AJ72G and NNX16AB77G. The help from the Theoretical Astrophysics Program of the University of Arizona is gratefully acknowledged.

References

Axford W I, Leer E and Skadron G 1977 *Proc. 15th Int. Cosmic Ray Conf.* (Plovdiv, Bulgaria, 1977), **11** 132-7
Bell A R 1978 *MNRAS* **182** 147
Blandford A D and Ostriker J P 1978 *Astrophys. J.* **221L** 29
Bieber J W and Chen J 1991 *Astrophys. J.* **372** 301
Burger R A, Moraal H and Webb G M 1985 *Astrophys. Space Sci.* **116** 107
Burger R A and Potgieter M S 1989 *Astrophys. J.* **339** 501
Burger R A and Hattingh M 1995 *Astrophys. J.* **230** 375
Chen J and Bieber J W 1993 *Astrophys. J.* **405** 375
Cummings A C, Stone E C and Webber W R 1987 *Geophys. Res. Lett.* **14** 174
Drake J F, Swisdak M and Opher M 2015 *Astrophys. J.* **808** 44
Florinski V and Pogorelov N V 2009 *Astropys. J.* **701** 642
Florinski V 2011 *Adv. Space Res.* **48** 308
Florinski V, Ferreira S E S and Pogorelov N V 2013 *Space Sci. Res.* **176** 147
Giacalone J, Jokipii J R and Kóta J 1999 *Proc. 26th Int. Cosmic Ray Conf.* (Salt Lake City, Utah, 1999), **7** 37
Gil A, Modzelewska R and Alania M V 2012 *Adv. Space Res.*, **50** 712
Hattingh M and Burger R A 1995 *Adv. Space Res.* **16** 9
Isenberg P A and Jokipii J R 1979 *Astrophys. J.* **234** 7431
Jokipii J R 1986 *J. Geophys. Res.* **91** 2929
Jokipii J R, Levy E H and Hubbard W B 1977 *Astrophys. J.* **213** 861
Jokipii J R and Kóta J 1989 *Geophys. Res. Lett.* **16** 1
Kóta J 1981 *Adv. Space Res.* **176** 391
Kóta J 1989 in *Physics of the Outer Heliosphere* Eds: S Grzedzielski and D E Page, Pergamon Press, COSPAR Colloquia Series **1** 119 - 31
Kóta J 2013 *Space Sci. Rev.* **176** 391
Kóta J and Jokipii J R 1983 *Astrophys. J.* **265** 573
Krimigis S M, Decker R B, Roelof E C, Hill M E, Armstrong T P, Gloeckler G, Hamilton D C and Lanzerotti L J 2013 *Science* **341** 144
Krymskii G F 1977 *Dokl. Akad. Nauk SSSR* **234** 1306
Luo Xi, Zhang M, Potgieter Marius, Feng Xueshang and Pogolerov N V. 2013 *Astrophys. J.* **808** 82L
Minnie J, Bieber J W, Matthaeus W H and Burger, R A 2007 *Astrophys. J.* **670** 1149
Moraal H 2013 *Space Sci. Rev.* **176** 299
Munakata K, Kozai M, Kato C and Kóta J 2014 *Astrophys. J.* **791** 22
Opher M, Drake J F, Zieger B and Gombosi T I 2015 *Astrophys J* **800** 280
Parker E N 1965 *Planet. Space Sci.* **13** 9
Pogorelov N V, Borovikov S N, Heerikhuisen J and Zhang M 2015 *Astrophys. J.* **812** 6
Potgieter M S 2013 *Space Sci. Rev.* **176** 165
Potgieter M S and Moraaal H 1985 *Space Sci. Rev.* **294** 425
Stone E C, Cummings A C, McDonald F B, Heikkila B C, Lal N and Webber W R 2013 *Science* **341** 150
Strauss R D, Potgieter M S, Ferreira S E S, Fichtner J and Scherer K 2013 *Astrophys. J.* **765** 91
Webber W R and Higbie P R 2009 *J. Geophys. Res.* DOI: 1029/2008JA013689